

Strong Charge-Transfer Chromophores from [2+2] Cycloadditions of TCNE and TCNQ to Peripheral Donor-Substituted Alkynes

Songhua Chen,^[a,b] Yongjun Li,^{*[a]} Chao Liu,^[a,b] Wenlong Yang,^[a,b] and Yuliang Li^{*[a]}

Keywords: Donor–acceptor systems / Cycloaddition / Charge transfer / Aggregate morphology

Peripheral donor-substituted *N,N*-dimethyl-4-[(7-nitrobenzo[*c*][1,2,5]thiadiazol-4-yl)ethynyl]aniline (**1a**), 4-(benzo[*c*][1,2,5]thiadiazol-4-ylethynyl)-*N,N*-dimethylaniline (**1b**), and 4,4'-[benzo[*c*][1,2,5]thiadiazole-4,7-diylbis(ethyne-2,1-diyl)]bis(*N,N*-dimethylaniline) (**2**) were prepared by Sonogashira cross-coupling reactions. Compounds **1a**, **1b**, and **2** subsequently reacted with tetracyanoethylene (TCNE) or 7,7,8,8-tetracyanoquinodimethane (TCNQ) to afford the charge-transfer chromophores **3–8**. X-ray crystallographic

analysis revealed the nonplanarity of these donor–acceptor (D–A) chromophores. Cyclic voltammetry (CV) exhibited a multistep reduction wave. UV/Vis spectra and theoretical calculations identified efficient intramolecular charge-transfer interactions. Moreover, scanning electron microscopy (SEM) showed the morphology transition and reconstruction process of **5** from 0D hollow nanospheres to 1D tubular microstructures.

Introduction

Over recent decades, push–pull chromophores (D– π –A) with strong electron donors (D) connected by π -conjugated spacers to strong electron acceptors (A) have been investigated because of their promising optoelectronic properties, such as large second- and third-order nonlinear optical effects.^[1] Appropriate choices of the D and A units has led to new high-performance molecular materials such as dye-sensitized solar cells, light-energy conversion, optical devices, and sensors.^[2] Furthermore, D–A-substituted conjugated molecules are highly polarized, intramolecular charge-transfer (ICT) compounds, which can be used to construct low-dimensional organic nanostructures^[3] and provide possibilities for the design and fabrication of well-defined, morphology-controlled nanostructures with desirable sizes, shapes, and functions. Low-dimensional supramolecular micro- or nanostructures have been successfully constructed from low-molecular-weight D–A-substituted ICT compounds with the help of D–A dipole–dipole interactions.^[3a–3c,4]

As strong electron acceptors, tetracyanoethylene (TCNE) and 7,7,8,8-tetracyanoquinodimethane (TCNQ) are of interest in the fabrication of optical and electrical recording,^[5] energy and data storage,^[6] sensors,^[7] and electrochromic and magnetic devices.^[8] Their derivatives have

been seen to form charge-transfer (CT) complexes^[9] and salts,^[10] some of which exhibit high electronic conductivity and magnetic phenomena.^[11] It has been reported that the reaction of electron-rich alkynes with TCNE afforded [2+2] cycloaddition products, which gave 1,1,4,4-tetracyano-1,3-butadienes (TCBD) in high to quantitative yields.^[12]

Herein, we show the fast [2+2] cycloaddition reaction of TCNE/TCNQ to alkynes substituted by electron-donating and electron-withdrawing groups, where the donor consists of *N,N*-dimethylaniline units, and benzothiadiazole or nitro groups function as the acceptor. Their structures have been characterized by X-ray crystallography, optical absorption spectroscopy, electrochemistry, and theoretical calculations. We have also utilized strong D–A dipole–dipole interactions as the main driving force to direct the growth of tubular microstructures.^[13]

Results and Discussion

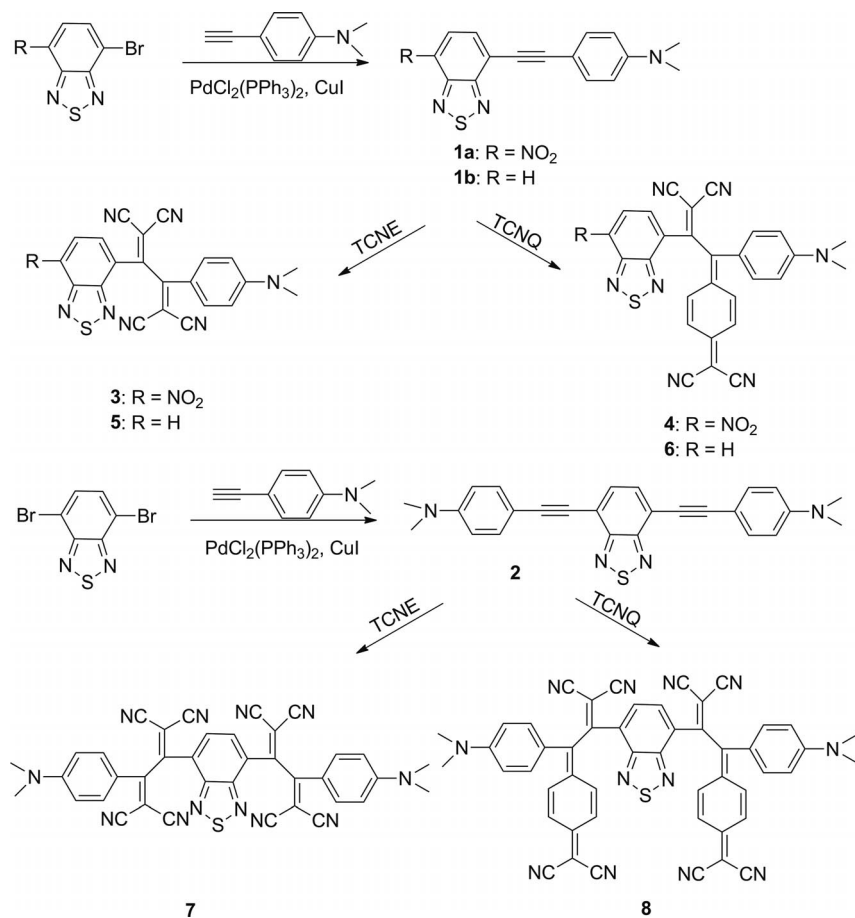
Synthesis

The synthesis of the CT chromophores **3–8** is outlined in (Scheme 1). 4-bromobenzo[*c*][1,2,5]thiadiazole, 4-bromo-7-nitrobenzo[*c*][1,2,5]thiadiazole and 4,7-dibromobenzo[*c*][1,2,5]thiadiazole were prepared according to literature methods.^[14] Standard Sonogashira coupling gave monoadducts *N,N*-dimethyl-4-[(7-nitrobenzo[*c*][1,2,5]thiadiazol-4-yl)ethynyl]aniline (**1a**) and 4-(benzo[*c*][1,2,5]thiadiazol-4-ylethynyl)-*N,N*-dimethylaniline (**1b**) in 83 and 65% isolated yield, respectively. Bisadduct 4,4'-[benzo[*c*][1,2,5]thiadiazole-4,7-diylbis(ethyne-2,1-diyl)]bis(*N,N*-dimethylaniline) (**2**) was also synthesized in a similar Pd-catalyzed reaction in 45% yield.^[15] Compounds **1** and **2** were subsequently

[a] Beijing National Laboratory for Molecular Sciences (BNLMS), CAS Key Laboratory of Organic Solids, Institute of Chemistry, Chinese Academy of Sciences, Beijing 100190, P. R. China
E-mail: ylli@iccas.ac.cn; liyj@iccas.ac.cn

[b] Graduate University of Chinese Academy of Sciences, Beijing 100049, P. R. China

Supporting information for this article is available on the WWW under <http://dx.doi.org/10.1002/ejoc.201101009>.



Scheme 1. Synthesis of 3–8.

used for the reaction with TCNE/TCNQ to give the desired products 3–8. A previous report^[12b] has shown that the reaction of TCNE with *N,N*-dimethylanilino (DMA)-substituted alkynes could reach almost quantitative yield (97%) by [2+2] cycloaddition. Similar reactions were carried out with 1a and 1b to yield the corresponding adducts 3 (78%) and 5 (83%), respectively, at room temperature. Likewise, the reaction of 2 with TCNE afforded 7 in 91% yield (Scheme 1).

In contrast to TCNE, TCNQ displays reduced reactivity in formal cycloadditions with alkynes. Compounds 4 (27%), 6 (20%), and 8 (35%) were obtained in low yields even with prolonged reaction times, elevated temperatures (60 °C) or excess TCNQ. The low yields observed are attributed to steric effects.

Identification of 3–8 was confirmed by NMR spectroscopy, MS, and elemental analysis. The ¹³C NMR spectrum of 7 was not obtained because of its low solubility. Compounds 3–8 are stable, deeply colored, and show no decomposition even after several weeks at room temperature.

X-ray Structure and Bond-Length Alternation

A single crystal of 5 (Figure 1a) was obtained by slow diffusion of *n*-hexane into a CH₂Cl₂ solution at room tem-

perature, and a solution containing 7 in CHCl₃ was concentrated slowly at room temperature to yield a crystal of 7 (Figure 1b). Compound 7 was found to cocrystallize with 1 equiv. of CHCl₃. Crystallographic data for both molecules are collected in Table S2 (Supporting Information).

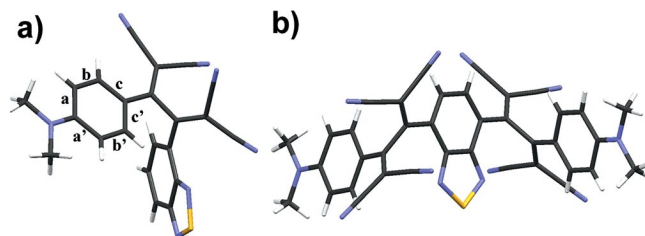


Figure 1. Molecular structures of 5 (a) and 7 (b). Solvent molecules were omitted for clarity in (b).

The X-ray crystal structures of 5 and 7 are nonplanar due to the strong repelling contacts between the benzothiadiazole moiety and TCBD group. The TCBD moieties of 7 are distorted with an angle of 38.5° relative to the neighboring benzene rings in the benzothiadiazole moiety, whereas the TCBD moiety of 5 has a torsion angle of 54.7°.

The crystal-packing diagrams show several interesting short intermolecular contacts. In the crystal-packing arrangement of 5 (Figure S1a, Supporting Information), multiple CN⋯CN interactions [$d(\text{N}3\cdots\text{C}9') = 3.11 \text{ \AA}$,

$d(\text{N}3\cdots\text{C}10') = 3.18 \text{ \AA}$] between two neighboring molecules are formed, as previously observed.^[16] Furthermore, the DMA residues of two neighboring molecules undergo antiparallel stacking at intermolecular $\text{C}\cdots\text{H}$ distances of around 2.90 \AA . The polarized N atoms of a CN moiety in one molecule interact with a neighboring benzothiadiazole ring, which plays an important role in the face-to-face packing. As can be seen from Figure S1b (Supporting Information), the conformation of **7** is locked and stabilized not only by the strong CN dipoles but also by a large number of intermolecular hydrogen bonds. The hydrogen bonds and $\text{CH}-\pi$ interactions, such as $\text{C}17\cdots\text{H}18'$, $\text{N}3\cdots\text{H}19'$, and $\text{C}17-\text{H}17\cdots\text{N}3''$, work cooperatively to help the DMA residues form antiparallel stacks. In addition, a remarkable feature of the crystal structure is that the CN groups of one molecule interact with the $\text{C}(\text{CN})_2$ moieties of the neighboring molecule. In this alignment, the CN group can form two $\text{CN}\cdots\text{CN}$ contacts [$d(\text{N}4\cdots\text{C}11'') = 3.22 \text{ \AA}$, $d(\text{N}4\cdots\text{C}9'') = 3.10 \text{ \AA}$, $d(\text{N}4\cdots\text{C}10'') = 3.18 \text{ \AA}$].

Bond-length alternation in the benzene ring of *N,N*-dimethylaniline is a good indicator for the efficiency of CT conjugation from the donor to the benzothiadiazole acceptor, which can be expressed by the quinoid character (δ_r) [Equation (1)].^[17]

$$\delta_r = \{[(a + a')/2 - (b + b')/2] + [(c + c')/2 - (b + b')/2]\}/2 \quad (1)$$

In benzene, the δ_r value is 0 (see Figure 1a for the definition of the bonds a , a' , b , b' , c , c'). Calculating from the X-ray crystal structures, **7** exhibits a δ_r value of 0.044, and **5** shows a similar value of 0.045. It has been reported that TCBD compounds with two different molecules in the unit cell exhibit an average δ_r value of 0.036,^[12b] and some DMA-substituted cyanoethynylethenes with strong D–A interactions display δ_r values of 0.033–0.037.^[18] Taking this into account, **5** and **7** exhibit efficient ICT interactions in which the benzothiadiazole moiety plays an important role.

UV/Vis Spectroscopy

The D–A systems are dark or black metallic solids, which are stable at ambient temperature. The UV/Vis spectra recorded in CH_2Cl_2 show multi-ICT bands (Figure 2, Table 1), which result from different D–A transitions. For example, **5** displays an intense band with $\lambda_{\text{max}} = 441 \text{ nm}$ and one weak shoulder at $\lambda_{\text{max}} = 550 \text{ nm}$. In contrast, the lower energy of the CT band of **3** with an apparent λ_{max} value of 472 nm clearly reflects the strong D–A interaction as the result of the insertion of the nitro group, and the absorbance at about 358 nm is assigned to the $\pi \rightarrow \pi^*$ transition of the benzothiadiazole unit.^[19] Similarly, **7** has a CT shoulder at about 647 nm with ϵ values 2.5 times larger than that of monomeric **5**. The highest occupied molecular orbital (HOMO) and lowest unoccupied molecular orbital (LUMO) from the calculation are depicted in Figure 3. It can be seen from the calculated spatial distributions that the density in the HOMO is concentrated in the DMA moiety, and the density in the LUMO on the TCBD and benzo-

thiadiazole units. The longer wavelength absorption is mainly from the HOMO–LUMO transition. It is worth noting that the energies of the HOMO-1 and HOMO are almost equal in **7**, which may be the cause for the larger absorption coefficients compared with those in **5**.

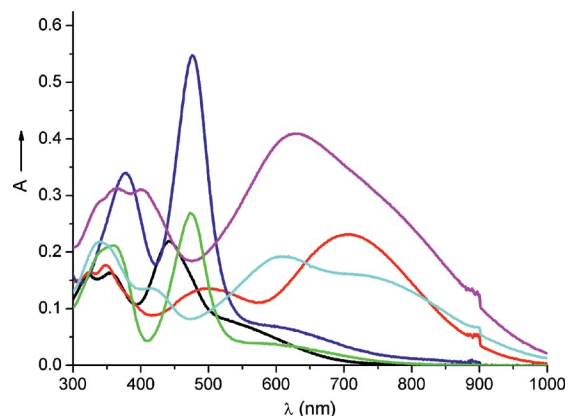


Figure 2. UV/Vis spectra of **3–8** in CH_2Cl_2 (green: **3**; cyan: **4**; black: **5**; red: **6**; blue: **7**; magenta: **8**).

Table 1. Summary of the UV/Vis spectra of **3–8** in CH_2Cl_2 .

Compound	λ_{max} [nm] ($\log \epsilon$) ^[a]	λ_{end} [nm]
3	358 (4.32), 472 (4.43)	760
4	338 (4.34), 618 (4.28)	980
5	441 (4.34), 550 ^[b] (2.85)	660
6	499 (3.13), 720 (4.36)	910
7	378 (4.53), 476 (4.74), 647 ^[b] (2.73)	780
8	365 (4.50), 400 (4.49), 628 (4.61)	990

[a] Measured in $1 \times 10^{-5} \text{ M}$ solution. [b] Shoulder.

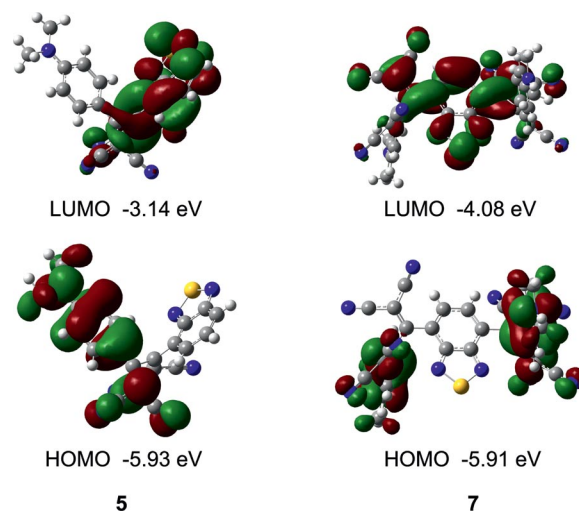


Figure 3. Calculated spatial distributions of the HOMO and LUMO for **5** and **7** [B3LYP/6-31G+(d,p)].

The TCNQ adduct **6** shifts the CT band to 499 nm , with a strong CT band of lower energy appearing at $\lambda_{\text{max}} = 720 \text{ nm}$ and $\lambda_{\text{end}} \approx 910 \text{ nm}$. Apart from the characteristic broad absorbance of **4** at 618 nm , the spectrum shows a new shoulder at a longer wavelength of 750 nm , which depends on more effective CT interactions. Solvatochromism

is a characteristic behavior of dipolar molecules. The absorption bands of TCBD adducts have been reported to be redshifted in polar solvents and blueshifted in nonpolar ones.^[12b] We investigated the solvent effect on the CT bands of **4**, **6**, and **8** in solvents with different polarities. The results show that the absorbance maxima are highly dependent on the solvent polarity (Table S1, Supporting Information). The CT band of **8** in *N,N*-dimethylformamide (DMF), CH₃OH, CH₃CN, tetrahydrofuran (THF), and toluene was at 710, 694, 674, 632, and 602 nm, respectively.

Electrochemistry

The redox properties of **3–8** were studied by CV in CH₂Cl₂ with *n*Bu₄NPF₆ (0.1 M) as the supporting electrolyte. The redox potentials vs. Fc⁺/Fc are listed in Table 2.

Table 2. CV of **3–8** in CH₂Cl₂ (+0.1 M *n*Bu₄NPF₆).^[a]

Compound	E_{ox}^1 [V]	E_{red}^1 [V]	E_{red}^2 [V]	E_{red}^3 [V]	E_{red}^4 [V]	E_{red}^5 [V]
3	0.82	-0.70	-0.93	-1.43	-1.83	–
4	0.33	-0.62	-0.79	-1.41	-2.08	–
5	0.73	-0.96	-1.36	-2.46	–	–
6	0.25	-0.75	-0.91	-2.28	–	–
7	0.73	-0.67	-0.83	-1.64	–	–
8	0.23	-0.64	-0.76	-0.80	-0.94	-2.57

[a] All potentials are given vs. Fc⁺/Fc (scan rate $\nu = 0.1 \text{ V s}^{-1}$).

The DMA donor in **3–8** undergoes an irreversible oxidation step with the potential ranging from 0.23 to 0.82 V. Bisadducts **7** and **8** have a single oxidation process, which can be assigned to the simultaneous one-electron oxidation of the two DMA units. This may be due to the noncoplanarity of the central 4,7-disubstituted benzothiadiazole ring and results in negligible electronic interactions between the DMA units.^[20] The oxidation potential was not significantly affected in either the monoadducts (0.73 V for **5** and **7**) or the bisadducts (0.25 and 0.23 V for **6** and **8**, respectively). On the other hand, the oxidation potential observed in **3** ($E_{\text{ox}} = +0.82 \text{ V}$) is more positive than that of **5** ($E_{\text{ox}} = +0.73 \text{ V}$), which indicates that the DMA unit in **5** is more electron-rich than that in **3**. The TCNQ adducts **4** ($E_{\text{ox}} = +0.33 \text{ V}$), **6** ($E_{\text{ox}} = +0.25 \text{ V}$), and **8** ($E_{\text{ox}} = +0.23 \text{ V}$) are oxidized at lower potentials compared to those of the TCNE adducts **5** and **7** ($E_{\text{ox}} = +0.73 \text{ V}$). The difference between the oxidation potentials of **3–8** suggests that the interactions between the donor and the acceptor groups are strong in the ground state.^[21]

Noticeably, these chromophores show multireversible reduction steps centered on the C(CN)₂ group as well as the benzothiadiazole moiety. Electrochemical reduction of **5** showed a reversible three-stage reduction wave at -0.96, -1.36, and -2.46 V. The first and second negative potentials are attributed to the E_{red} values of the TCBD group, and the third is attributed to the E_{red} value of the benzothiadiazole unit.^[22] Compared with **5**, **3** exhibits another reduction at -1.43 V, probably due to the reduction of the nitro group,^[23] which was also observed in **4** (-1.41 V). The intro-

duction of the strongly accepting nitro group in **3** facilitated the reduction of the benzothiadiazole moiety ($E_{\text{red}}^4 = -1.83 \text{ V}$) compared to **5** ($E_{\text{red}}^3 = -2.46 \text{ V}$) with a 630 mV shift. This indicates that the nitro-modified benzothiadiazole moiety in **3** is more electron-deficient than the benzothiadiazole group in **5**. Similarly, there is a 200 mV shift between **4** ($E_{\text{red}}^4 = -2.08 \text{ V}$) and **6** ($E_{\text{red}}^3 = -2.28 \text{ V}$) in the benzothiadiazole moiety reduction step. Furthermore, the first and second reversible reduction steps became notably facilitated by the introduction of the nitro group. As observed by Diederich and co-workers,^[1b] each TCBD moiety can accommodate two electrons. Thus, dimeric **7** with two TCBD moieties accepted four electrons in two reversible two-electron reduction steps at -0.67 and -0.83 V. The first reduction potentials of **5** and **7** decreased as the number of TCBD units increased. This indicates that the TCBD unit reduces the LUMO level and increases the π -accepting ability.^[24] The electrochemical reduction of **8** exhibited a reversible reduction wave, whose potentials were identified at -0.64, -0.76, -0.80, -0.94, and -2.57 V by CV, which are attributed to the formation of a pentaanionic species.

Aggregate Structures of **5**

Figure 4 shows typical SEM images of the aggregate nanostructures of **5** with different morphologies. The preparation of nanostructures was carried out by a simple solution process. Compound **5** was dissolved in THF at a concentration of $2.0 \times 10^{-3} \text{ M}$. Then, 1 mL of the solution was injected into 5 mL of vigorously stirred hexane (antisolvent) at 30 °C. Immediately after the injection, one drop of the suspension was put onto a silicon substrate for SEM examination (Figure 4a). Large spherical particles with diameters ranging from 0.5 to 1.5 μm were observed in the SEM images. A large number of membrane defects on the spherical structures was also observed. After stirring for 3 min, a drop of suspension was put on to a silicon substrate, and the morphology was measured in situ (Figure 4b). We found that the wall of the sphere had collapsed, and the hollow nature of the structure is observable. SEM (Figure 4c) was used to observe the sample obtained after 30 min. The result showed that a 1D hollow aggregate structure was formed with lengths over 5 μm , which clearly demonstrates that the solvent strongly favors not only the formation of a large-scale spherical aggregate structure but also a 1D hollow aggregate structure. The driving forces for the self-organization of spherical and hollow structures of **5** are mainly intermolecular interactions. The growth and assembly process can be proposed as follows: when the solution of **5** in THF was injected into hexane, the solvent polarity and the chemical environment of the molecules was changed and formed the spherical aggregate. During concentration, the THF solution was lost from the spherical shell, which left defects. The vesicles formed initially had a high curvature, and their fusion could release curvature energy, which would lead to a thermodynamically more stable structure.^[3a,21] Therefore, a hemispherical structure was

formed in which the molecules flowed with the solvent and aggregated along the initial opening hole. In the growth process to form the hollow tubular microstructures, the strong intermolecular interactions observed in the crystal packing are proposed to act as the driving force for the molecules to aggregate, as confirmed by similar X-ray diffraction patterns between the aggregate and the crystal (Figure 4d).^[3c,25]

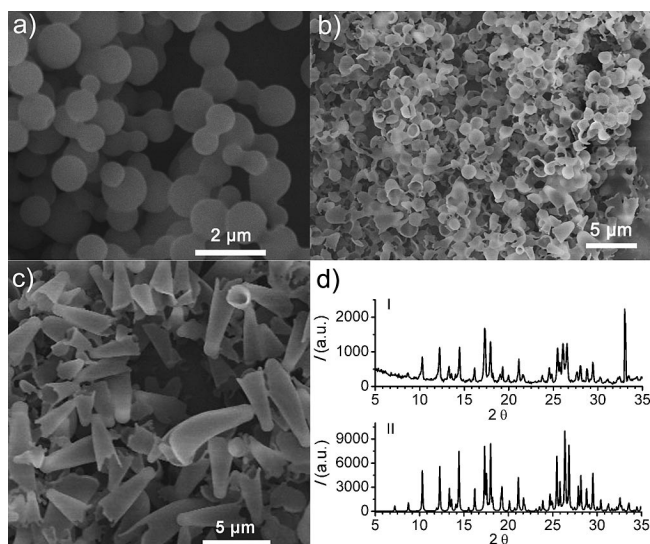


Figure 4. SEM images of **5** prepared at different ageing times in THF/hexane. (a) immediately, (b) after 3 min, (c) after 30 min; (d) compares the XRD patterns of the aggregate (I) and the crystal (II) of **5**.

The THF solution was essential for this kind of tubular formation progress. When the sample was dissolved in CH_2Cl_2 (Figure S21, Supporting Information), a 3D network of the flexible endless fibers was formed. Furthermore, when CH_2Cl_2 was used instead of THF, the changes in morphology were not as obvious in the mixture with hexane.

Except **5**, the other compounds with bulkier substituents do not form well-defined aggregate structures. This indicated that the molecular structure, which controls the packing style, plays as important a role as the dipole–dipole interaction in directing the aggregation.

Conclusions

Three peripheral donor-substituted alkynes (**1a**, **1b**, and **2**) were prepared by Sonogashira cross-coupling reactions and subsequently used in reactions with TCNE or TCNQ to give **3–8**. X-ray crystallographic analysis (for **5** and **7**) revealed the nonplanarity of these D–A chromophores. CV showed that **3–8** exhibit multistep reduction waves. UV/Vis spectra and theoretical calculations identified the efficient ICT interactions. The aggregate structures of **5** were investigated by SEM, and spherical and hollow structures were formed in the controlled assembly process. These optical and electronic features make them potentially useful for fu-

ture applications in devices. The exploration of optical nonlinearities of the TCNE and TCNQ derivatives is currently underway.

Experimental Section

Materials and Characterization: Most of the chemical reagents were purchased from Alfa Aesar and Aldrich Chemicals and were used as received unless indicated otherwise. All solvents were purified by using standard procedures. Column chromatography was performed on silica gel (size 200–300 mesh). ^1H and ^{13}C NMR spectra were recorded with a Bruker ARX400 spectrometer. UV/Vis spectra were measured with a Hitachi U-3010 spectrometer. Organic nanostructures were prepared by a simple solution process. 4-Bromobenzo[*c*][1,2,5]thiadiazole, 4-bromo-7-nitrobenzo[*c*][1,2,5]thiadiazole and 4,7-dibromobenzo[*c*][1,2,5]thiadiazole were synthesized according to previously described procedures.^[14]

General Procedure for the Synthesis of *N,N*-Dimethyl-4-[(7-nitrobenzo[*c*][1,2,5]thiadiazol-4-yl)ethynyl]aniline (1a**):** To a stirred solution of 4-ethynyl-*N,N*-dimethylbenzenamine (290 mg, 2.0 mmol) and 4-bromo-7-nitrobenzo[*c*][1,2,5]thiadiazole (518 mg, 2.0 mmol) in THF and (*i*Pr)₂NH (3:1, v/v) were added $\text{PdCl}_2(\text{PPh}_3)_2$ (40 mg) and CuI (20 mg) under an argon flow at room temperature. The mixture was stirred at room temperature for 1 h. The solvent was evaporated under reduced pressure, and the mixture was purified by SiO_2 chromatography with CH_2Cl_2 /petroleum ether (1:2, v/v) to obtain **1a** (538 mg, 83%) as a yellow powder. ^1H NMR (400 MHz, CDCl_3): δ = 3.06 (s, 6 H), 6.72 (d, J = 8.6 Hz, 2 H), 7.58 (d, J = 8.8 Hz, 2 H), 7.79 (m, J = 8.0 Hz, 1 H), 8.59 (d, J = 8.0 Hz, 1 H) ppm. ^{13}C NMR (100 MHz, CDCl_3): δ = 155.9, 151.4, 146.7, 137.6, 134.1, 128.6, 126.1, 111.8, 107.8, 106.0, 85.1, 40.2 ppm. HRMS: calcd. for $[\text{M}]^+$ 324.0681; found 324.0686. $\text{C}_{16}\text{H}_{12}\text{N}_4\text{O}_2\text{S}$ (324.36): calcd. C 59.25, H 3.73, N 17.27; found C 69.17, H 3.75, N 17.20.

4-(Benzo[*c*][1,2,5]thiadiazol-4-ylethynyl)-*N,N*-dimethylaniline (1b**):** To a stirred solution of 4-ethynyl-*N,N*-dimethylbenzenamine (522 mg, 3.6 mmol) and 4-bromobenzo[*c*][1,2,5]thiadiazole (642 mg, 3.0 mmol) in THF and (*i*Pr)₂NH (3:1, v/v) were added $\text{PdCl}_2(\text{PPh}_3)_2$ (40 mg) and CuI (20 mg) under an argon flow at room temperature. The reaction mixture was heated to reflux with stirring for 10 h, and then cooled to room temperature. The solvent was then evaporated under reduced pressure, and the mixture was purified by SiO_2 chromatography with CH_2Cl_2 /petroleum ether (1:3, v/v) to obtain **1b** (544 mg, 65%) as a yellow powder. ^1H NMR (400 MHz, CDCl_3): δ = 3.02 (s, 6 H), 6.69 (d, J = 8.8 Hz, 2 H), 7.54 (d, J = 5.4 Hz, 2 H), 7.58 (m, J = 7.2 Hz, 1 H), 7.74 (d, J = 7.0 Hz, 1 H), 7.93 (d, J = 8.8 Hz, 1 H) ppm. ^{13}C NMR (100 MHz, CDCl_3): δ = 154.9, 154.8, 150.6, 133.4, 131.8, 129.5, 120.8, 118.3, 111.8, 109.3, 97.9, 83.7, 40.3 ppm. EI-MS: m/z = 279 $[\text{M}]^+$. $\text{C}_{16}\text{H}_{13}\text{N}_3\text{S}$ (279.36): calcd. C 68.79, H 4.69, N 15.04; found C 68.60, H 4.69, N 14.87.

4,4'-[Benzo[*c*][1,2,5]thiadiazole-4,7-diylbis(ethyne-2,1-diyl)]bis(*N,N*-dimethylaniline) (2**):** To a stirred solution of 4-ethynyl-*N,N*-dimethylbenzenamine (870 mg, 6.0 mmol) and 4,7-dibromobenzo[*c*][1,2,5]thiadiazole (882 mg, 3.0 mmol) in THF and Et_3N (3:1, v/v) were added $\text{PdCl}_2(\text{PPh}_3)_2$ (40 mg) and CuI (20 mg) under a nitrogen flow. The reaction mixture was heated to reflux with stirring for 10 h before the solvent was evaporated. The mixture was purified by SiO_2 chromatography with CH_2Cl_2 /petroleum ether (2:1, v/v) to obtain **2** (569 mg, 45%) as a red powder. ^1H NMR (400 MHz, CDCl_3): δ = 3.02 (s, 12 H), 6.68 (d, J = 8.9 Hz, 4 H), 7.54 (d, J = 8.9 Hz, 4 H), 7.70 (s, 2 H) ppm. ^{13}C NMR (100 MHz,

CDCl_3): $\delta = 154.6, 150.6, 133.4, 131.8, 117.1, 111.8, 109.3, 99.2, 84.3, 40.3$ ppm. EI-MS: $m/z = 422$ $[\text{M}]^+$. $\text{C}_{26}\text{H}_{22}\text{N}_4\text{S}$ (422.55): calcd. C 73.90, H 5.25, N 13.26; found C 73.69, H 5.25, N 12.94.

2-[4-(Dimethylamino)phenyl]-3-(7-nitrobenzo[c][1,2,5]thiadiazol-4-yl)buta-1,3-diene-1,1,4,4-tetracarbonitrile (3): TCNE (64 mg, 0.5 mmol) was added to a solution of **1a** (162 mg, 0.5 mmol) in CH_2Cl_2 (20 mL). The mixture was stirred at room temperature for 1 h. The solvent was removed in vacuo, and the product was purified by SiO_2 chromatography with CH_2Cl_2 as the eluent to yield **3** as a dark brown solid (165 mg, 78%). M.p. 136 °C. ^1H NMR (400 MHz, CDCl_3): $\delta = 3.14$ (s, 6 H), 6.68 (d, $J = 9.2$ Hz, 2 H), 7.78 (d, $J = 9.2$ Hz, 2 H), 8.11 (d, $J = 7.9$ Hz, 1 H), 8.59 (d, $J = 7.9$ Hz, 1 H) ppm. ^{13}C NMR (100 MHz, CDCl_3): $\delta = 163.2, 161.8, 154.5, 152.6, 146.5, 141.8, 132.8, 130.9, 130.6, 126.0, 118.0, 114.0, 113.7, 112.3, 111.0, 110.3, 95.5, 75.9, 40.2$ ppm. HRMS: calcd. for $[\text{M}]^+$ 425.0804; found 452.0810.

2-[4-(3,3-Dicyano-1-((4-(dimethylamino)phenyl)-2-(7-nitrobenzo[c][1,2,5]thiadiazol-4-yl)allylidene)cyclohexa-2,5-dien-1-ylidene]malononitrile (4): TCNQ (102 mg, 0.5 mmol) was added to a solution of **1a** (162 mg, 0.5 mmol) in THF (40 mL). The mixture was stirred for 20 h at 60 °C. The solvent was removed in vacuo, and the product was purified by SiO_2 chromatography with $\text{CH}_2\text{Cl}_2/\text{CH}_3\text{OH}$ (100:1) as the eluent to yield **4** as a dark black solid (71 mg, 27%). M.p. 145 °C. ^1H NMR (400 MHz, CDCl_3): $\delta = 3.07$ (s, 6 H), 6.59 (d, $J = 8.8$ Hz, 2 H), 7.21 (d, $J = 8.9$ Hz, 2 H), 7.29 (d, $J = 5.1$ Hz, 2 H), 7.34 (m, 2 H), 7.92 (d, $J = 7.8$ Hz, 1 H), 8.52 (d, $J = 7.8$ Hz, 1 H) ppm. ^{13}C NMR (100 MHz, CDCl_3): $\delta = 166.3, 153.8, 152.9, 152.8, 150.1, 146.4, 141.2, 136.1, 134.5, 134.3, 134.2, 129.9, 129.3, 126.2, 126.0, 125.8, 122.4, 114.5, 114.4, 112.3, 112.0, 111.5, 94.0, 73.4, 40.1$ ppm. HRMS: calcd. for $[\text{M}]^+$ 528.1117; found 528.1122.

2-(Benzo[c][1,2,5]thiadiazol-4-yl)-3-[4-(dimethylamino)phenyl]buta-1,3-diene-1,1,4,4-tetracarbonitrile (5): TCNE (64 mg, 0.5 mmol) was added to a solution of **1b** (140 mg, 0.5 mmol) in CH_2Cl_2 (40 mL). The mixture was stirred at room temperature for 1 h. The solvent was removed in vacuo, and the product was purified by SiO_2 chromatography with CH_2Cl_2 as the eluent to yield **5** as a dark brown solid (169 mg, 83%). M.p. 196 °C. ^1H NMR (400 MHz, CDCl_3): $\delta = 3.12$ (s, 6 H), 6.67 (d, $J = 9.1$ Hz, 2 H), 7.75 (t, $J = 7.9$ Hz, 1 H), 7.81 (d, $J = 9.1$ Hz, 2 H), 8.02 (d, $J = 7.1$ Hz, 1 H), 8.26 (d, $J = 8.8$ Hz, 1 H) ppm. ^{13}C NMR (100 MHz, CDCl_3): $\delta = 165.4, 163.4, 155.0, 154.4, 151.0, 132.9, 132.6, 128.9, 127.4, 125.6, 118.6, 114.5, 113.9, 112.2, 111.8, 111.2, 92.8, 75.9, 40.3$ ppm. HRMS: calcd. for $[\text{M}]^+$ 407.0953; found 407.0959. $\text{C}_{16}\text{H}_{13}\text{N}_3\text{S}$ (279.36): calcd. C 64.85, H 3.22, N 24.06; found C 64.70, H 3.28, N 24.19.

2-[1-(Benzo[c][1,2,5]thiadiazol-4-yl)-2-(4-(dicyanomethylene)cyclohexa-2,5-dienylidene)-2-(4-(dimethylamino)phenyl)ethylidene]malononitrile (6): TCNQ (102 mg, 0.5 mmol) was added to a solution of **1b** (107 mg, 0.5 mmol) in CH_2Cl_2 (40 mL). The mixture was stirred at room temperature for 30 h. The solvent was removed in vacuo, and the product was purified by SiO_2 chromatography with CH_2Cl_2 as the eluent to yield **6** as a dark black solid (48 mg, 20%). M.p. 244 °C. ^1H NMR (400 MHz, CDCl_3): $\delta = 3.08$ (s, 6 H), 6.63 (d, $J = 8.7$ Hz), 7.19 (d, $J = 9.4$ Hz, 1 H), 7.28 (m, 4 H), 7.41 (d, $J = 9.6$ Hz, 1 H), 7.67 (t, $J = 7.8$ Hz, 1 H), 7.81 (d, $J = 6.9$ Hz, 1 H), 8.17 (d, $J = 8.7$ Hz, 1 H) ppm. ^{13}C NMR (100 MHz, CDCl_3): $\delta = 168.9, 154.9, 154.2, 152.9, 151.9, 151.3, 136.4, 134.9, 134.7, 133.6, 131.9, 128.8, 126.4, 125.7, 125.3, 123.6, 114.8, 114.7, 112.7, 112.3, 112.1, 92.3, 72.6, 40.3$ ppm. MS: $m/z = 483$ $[\text{M}]^+$. $\text{C}_{28}\text{H}_{17}\text{N}_7\text{S}$ (483.55): calcd. C 69.55, H 3.54, N 20.28; found C 69.43, H 3.52, N 20.18.

3,3'-(Benzo[c][1,2,5]thiadiazole-4,7-diyl)bis[2-(4-(dimethylamino)phenyl)buta-1,3-diene-1,1,4,4-tetracarbonitrile] (7): TCNE (77 mg, 0.6 mmol) was added to a solution of **2** (126 mg, 0.3 mmol) in CH_2Cl_2 (60 mL) at room temperature. The mixture was stirred at room temperature for 30 min. The solvent was removed in vacuo, and the product was purified by SiO_2 chromatography with CH_2Cl_2 as the eluent to yield **7** as a dark green solid (185 mg, 91%). M.p. 301 °C. ^1H NMR (400 MHz, CDCl_3): $\delta = 3.14$ (s, 12 H), 6.68 (d, $J = 9.4$ Hz, 4 H), 7.76 (d, $J = 8.1$ Hz, 4 H), 8.05 (s, 2 H) ppm. MS (MALDI-TOF): 679.5 $[\text{M} + 1]^+$. HRMS: calcd. for $[\text{M}]^+$ 678.1811; found 678.1822.

2,2'-(Benzo[c][1,2,5]thiadiazole-4,7-diylbis[2-(4-(dicyanomethylene)cyclohexa-2,5-dien-1-ylidene)-2-(4-(dimethylamino)phenyl)ethyl-1-yl-1-ylidene])dimalononitrile (8): To a stirred solution of **2** (126 mg, 0.3 mmol) in CH_2Cl_2 (60 mL) was added TCNQ (122 mg, 0.6 mmol). The reaction mixture was heated to reflux with stirring for 48 h before the solvent was evaporated. The mixture was purified by SiO_2 chromatography with CH_2Cl_2 to obtain **8** (87 mg, 35%) as a dark black powder. M.p. 213 °C. ^1H NMR (400 MHz, CDCl_3): $\delta = 3.09$ (s, 12 H), 6.64 (d, $J = 8.4$ Hz, 4 H), 7.20 (d, $J = 7.3$ Hz, 2 H), 7.27 (m, 8 H), 7.38 (d, $J = 9.6$ Hz, 2 H), 7.76 (s, 2 H) ppm. ^{13}C NMR (100 MHz, CDCl_3): $\delta = 167.1, 153.9, 153.1, 151.4, 150.5, 136.1, 134.7, 134.3, 133.7, 132.1, 130.6, 126.0, 125.6, 122.7, 114.6, 112.5, 112.2, 111.7, 93.5, 73.2, 40.3$ ppm. MS (MALDI-TOF): $m/z = 831.6$. $\text{C}_{50}\text{H}_{30}\text{N}_{12}\text{S}$ (830.93): calcd. C 72.27, H 3.64, N 20.23; found C 72.35, H 3.60, N 19.94.

CCDC-814624 (for **5**) and -814625 (for **7**) contain the supplementary crystallographic data for this paper. These data can be obtained free of charge from The Cambridge Crystallographic Data Centre via www.ccdc.cam.ac.uk/data_request/cif.

Supporting Information (see footnote on the first page of this article): Cyclic voltammetry, molecular orbital and SEM images.

Acknowledgments

We are grateful for financial support from the National Nature Science Foundation of China (21031006, 20831160507, 20721061, and 90922017) and the National Basic Research 973 Program of China.

- [1] a) T.-G. Zhang, Y. Zhao, I. Asselberghs, A. Persoons, K. Clays, M. J. Therien, *J. Am. Chem. Soc.* **2005**, *127*, 9710–9720; b) M. Kivala, C. Boudon, J.-P. Gisselbrecht, P. Seiler, M. Gross, F. Diederich, *Angew. Chem.* **2007**, *119*, 6473; *Angew. Chem. Int. Ed.* **2007**, *46*, 6357–6360.
- [2] a) A. P. Kulkarni, C. J. Tonzola, A. Babel, S. A. Jenekhe, *Chem. Mater.* **2004**, *16*, 4556–4573; b) P. T. Furuta, L. Deng, S. Garon, M. E. Thompson, J. M. J. Fréchet, *J. Am. Chem. Soc.* **2004**, *126*, 15388–15389.
- [3] a) J. Xu, X. Liu, J. Lv, M. Zhu, C. Huang, W. Zhou, X. Yin, H. Liu, Y. Li, J. Ye, *Langmuir* **2008**, *24*, 4231–4237; b) X. Zhang, X. Zhang, K. Zou, C.-S. Lee, S.-T. Lee, *J. Am. Chem. Soc.* **2007**, *129*, 3527–3532; c) X. J. Zhang, X. H. Zhang, W. S. Shi, X. M. Meng, C. S. Lee, S. T. Lee, *Angew. Chem.* **2007**, *119*, 1547; *Angew. Chem. Int. Ed.* **2007**, *46*, 1525–1528; d) H. B. Liu, J. L. Xu, Y. J. Li, Y. L. Li, *Acc. Chem. Res.* **2010**, *43*, 1496–1508.
- [4] a) C. Zhang, X. Zhang, X. Zhang, X. Fan, J. Jie, J. C. Chang, C.-S. Lee, W. Zhang, S.-T. Lee, *Adv. Mater.* **2008**, *20*, 1716–1720; b) Y. Yamamoto, T. Fukushima, Y. Suna, N. Ishii, A. Saeki, S. Seki, S. Tagawa, M. Taniguchi, T. Kawai, T. Aida, *Science* **2006**, *314*, 1761–1764; c) J. Xu, L. Wen, W. Zhou, J. Lv, Y. Guo, M. Zhu, H. Liu, Y. Li, L. Jiang, *J. Phys. Chem. C* **2009**, *113*, 5924–5932.

- [5] H. Peng, Z. Liu, *Coord. Chem. Rev.* **2010**, *254*, 1151–1168.
- [6] C. Ran, H. Peng, W. Zhou, X. Yu, Z. Liu, *J. Phys. Chem. B* **2005**, *109*, 22486–22490.
- [7] a) T. J. Wooster, A. M. Bond, *Analyst* **2003**, *128*, 1386–1390; b) T. J. Wooster, A. M. Bond, M. J. Honeychurch, *Anal. Chem.* **2003**, *75*, 586–592.
- [8] D. F. Perepichka, M. R. Bryce, C. Pearson, M. C. Petty, E. J. L. McInnes, J. P. Zhao, *Angew. Chem.* **2003**, *115*, 4784; *Angew. Chem. Int. Ed.* **2003**, *42*, 4636–4639.
- [9] a) K. Tahara, T. Fujita, M. Sonoda, M. Shiro, Y. Tobe, *J. Am. Chem. Soc.* **2008**, *130*, 14339–14345; b) H. B. Liu, Q. Zhao, Y. L. Li, Y. Liu, F. S. Lu, J. P. Zhuang, S. Wang, L. Jiang, D. B. Zhu, D. P. Yu, L. F. Chi, *J. Am. Chem. Soc.* **2005**, *127*, 1120–1121.
- [10] M. Kivala, C. Boudon, J. P. Gisselbrecht, B. Enko, P. Seiler, I. B. Müller, N. Langer, P. D. Jarowski, G. Gescheidt, F. Diederich, *Chem. Eur. J.* **2009**, *15*, 4111–4123.
- [11] T. Akutagawa, T. Hasegawa, T. Nakamura, T. Inabe, G. Saito, *Chem. Eur. J.* **2002**, *8*, 4402–4411.
- [12] a) M. I. Bruce, J. R. Rodgers, M. R. Snow, A. G. Swincer, *J. Chem. Soc., Chem. Commun.* **1981**, 271–272; b) T. Michinobu, C. Boudon, J.-P. Gisselbrecht, P. Seiler, B. Frank, N. N. P. Moonen, M. Gross, F. Diederich, *Chem. Eur. J.* **2006**, *12*, 1889–1905; c) C. Cai, I. Liakatas, M.-S. Wong, M. Bösch, C. Bosshard, P. Günter, S. Concilio, N. Tirelli, U. W. Suter, *Org. Lett.* **1999**, *1*, 1847–1849; d) P. Reutenauer, M. Kivala, P. D. Jarowski, C. Boudon, J.-P. Gisselbrecht, M. Gross, F. Diederich, *Chem. Commun.* **2007**, 4898–4900.
- [13] J. Xu, H. Zheng, H. Liu, C. Zhou, Y. Zhao, Y. Li, Y. Li, *J. Phys. Chem. C* **2010**, *114*, 2925–2931.
- [14] a) K. Pilgram, M. Zupan, R. Skiles, *J. Heterocycl. Chem.* **1970**, *7*, 629–633; b) K. Pilgram, M. Zupan, *J. Org. Chem.* **1971**, *36*, 207–209.
- [15] S. Chen, Y. Li, W. Yang, N. Chen, H. Liu, Y. Li, *J. Phys. Chem. C* **2010**, *114*, 15109–15115.
- [16] J. L. Alonso-Gómez, P. Schanen, P. Rivera-Fuentes, P. Seiler, F. Diederich, *Chem. Eur. J.* **2008**, *14*, 10564–10568.
- [17] a) C. Dehu, F. Meyers, J. L. Bredas, *J. Am. Chem. Soc.* **1993**, *115*, 6198–6206; b) A. Hilger, J.-P. Gisselbrecht, R. R. Tykwin-ski, C. Boudon, M. Schreiber, R. E. Martin, H. P. Luthi, M. Gross, F. Diederich, *J. Am. Chem. Soc.* **1997**, *119*, 2069–2078.
- [18] N. N. P. Moonen, F. Diederich, *Org. Biomol. Chem.* **2004**, *2*, 2263–2266.
- [19] H. Zhang, X. Wan, X. Xue, Y. Li, A. Yu, Y. Chen, *Eur. J. Org. Chem.* **2010**, 1681–1687.
- [20] K. Danel, T.-H. Huang, J. T. Lin, Y.-T. Tao, C.-H. Chuen, *Chem. Mater.* **2002**, *14*, 3860–3865.
- [21] D. M. Vriezema, J. Hoogboom, K. Velonia, K. Takazawa, P. C. M. Christianen, J. C. Maan, A. E. Rowan, R. J. M. Nolte, *Angew. Chem.* **2003**, *115*, 796; *Angew. Chem. Int. Ed.* **2003**, *42*, 772–776.
- [22] H. Sakurai, M. T. S. Ritonga, H. Shibatani, T. Hirao, *J. Org. Chem.* **2005**, *70*, 2754–2762.
- [23] P. Allongue, M. Delamar, B. Desbat, O. Fagebaume, R. Hitmi, J. Pinson, J.-M. Savéant, *J. Am. Chem. Soc.* **1997**, *119*, 201–207.
- [24] T. Shoji, S. Ito, K. Toyota, M. Yasunami, N. Morita, *Chem. Eur. J.* **2008**, *14*, 8398–8408.
- [25] X. J. Zhang, X. H. Zhang, K. Zou, C. S. Lee, S. T. Lee, *J. Am. Chem. Soc.* **2007**, *129*, 3527–3532.

Received: July 12, 2011

Published Online: September 16, 2011